Abstract ID: A1586

SPIN-POLARIZATION IN FRACTIONAL QUANTUM HALL EFFECT

Shosuke Sasaki

Shizuoka Institute of Science and Technology, 2200-2 Toyosawa, Fukuroi 437-8555, Japan

Phone:+81-538-45-0191, Fax:+81-538-45-0110, E-mail: sasaki@ns.sist.ac.jp

Keywords: Equilibrium thermodynamics and statistical mechanics, Many body and quasi-particle theories, Hall effect, Magnetic phenomena, Quantum wells, Semiconductor-semiconductor heterostructures

Abstract

Experimental data show a number of plateaus of varying widths in the magnetic-field dependence of the electron-spin-polarization for fractional quantum Hall states. We have calculated the magnetic-field dependence of the spin-polarization using a new theory. We start by adopting the Landau gauge and ignoring Coulomb interactions between electrons; then we construct single electron states in equally spaced orbitals. For a number of filling factors we have examined the many-electron states with electron configurations having minimum classical Coulomb energy. The residual Coulomb interactions in each many-electron state produce spin-exchange-forces. We have solved the eigenvalue problem of the interaction Hamiltonian composed of nearest neighbor spin-exchange-interactions. From the eigenvalues we have calculated the magnetic-field dependence of the spin-polarization. Our results are in good accord with the magnetic-field dependence in experimental results, including the number and shape of the plateaus.

1. Introduction

The fractional quantum Hall effect (FQHE) has been the subject of a number of theoretical treatments [1, 2]**.** One theory is that of Tao and Thouless [2]**,** which we have developed in a previous paper to explain the energy gap in FQHE [3] and obtained results in good agreement with the experimental data of the Hall resistance [4]. In this paper we study the magnetic-field dependence of the spin-polarization. The electron spin polarizations of the fractional quantum Hall states have been measured by Kukushkin, Klitzing, and Eberl for twelve filling factors [5]. The data show various types of behaviors for the magnetic-field dependence of the electron spin polarization. For the filling factors 1/2, 1/4, 3/5, 3/7, 7/5, and 3/2, the spin polarization value is proportional to the magnetic field strength near zero field. On the other hand, for the filling factors 2/3, 4/7, 2/5, 4/9, 8/5, and 4/3, the magnitude of the spin polarization is nearly equal to zero within a range near zero magnetic field, indicating an energy gap for these filling factors. We explain these properties by solving the eigenvalue problem for the Hamiltonian including the spin exchange interactions between nearest neighbor electrons. The calculated curves display the same number of plateaus as observed in the experimental data, with the same width and height; that is to say, the present theory can satisfactorily explain the behaviors of the spin polarizations in the quantum Hall effect.

2. Many-electron states

We first discuss the single electron states for the quantum Hall Effect. As is well known, a single electron state under a magnetic field of strength *B* has the form of a plane wave in the *x*-direction and has a Gaussian function form in the *y*-direction;

$$\psi_k \equiv \psi_k(x,y,z) = u e^{ikx} e^{-\alpha(y-c)^2} \phi(z), \quad (1)$$

where $k = (2\pi/\ell)\times$ integer, $\alpha = eB/(2\hbar)$, $c = k\hbar/(eB)$, (2)

and ℓ is the length of the system in the *x*-direction. The interval between the values of *c* is $2\pi\hbar/(\ell eB)$ and therefore all orbitals are equally spaced.

We divide the total Hamiltonian H_{T} into two parts, $H_{\mathrm{T}} = H_{\mathrm{D}} + H_{\mathrm{I}}$, where the new 0^{th} order Hamiltonian H_{D} is the sum of three parts, the kinetic energy, the vector potential part of the magnetic field, and the classical Coulomb energy between electrons (the diagonal part of the Coulomb interaction). The residual part of the Coulomb interaction is denoted by H_{I}.

The 0^{th} order ground state takes an electron configuration so as to produce the minimum value of the classical Coulomb energy. We first consider the electron configuration for the filling factor ν=2/3 as an example. When the quantum orbitals are filled with electrons in the sequence (filled, filled, empty, filled, filled, empty, ...), the many-electron state possesses the minimum classical Coulomb energy because this sequence is the most uniform for ν=2/3 (see Figure 1).

----------Fig. 1 ----------

The many-electron state Ψ is

$$\Psi = \psi_{k_1}(x_1,y_1,z_1)\psi_{k_2}(x_2,y_2,z_2)\psi_{k_3}(x_3,y_3,z_3)\psi_{k_4}(x_4,y_4,z_4)\cdots, \quad (3)$$

where $k_2 = k_1 + 2\pi/\ell$, $k_3 = k_1 + 3\times 2\pi/\ell$, $k_4 = k_1 + 4\times 2\pi/\ell$, $k_5 = k_1 + 6\times 2\pi/\ell$ ... (4)

Numbering the electrons left to right in Figure 1, it can be seen that electrons 1 and 2 occupy nearest neighbor orbitals, whereas electrons 2 and 3 occupy second nearest orbitals as they are separated by an empty orbital. The difference in wave number between electrons in nearest neighbor orbitals is $2\pi/\ell$, e.g. $k_2 - k_1 = 2\pi/\ell$. The difference in wave number between electrons separated by an empty orbital is $2\times 2\pi/\ell$, e.g. $k_3 - k_2 = 2\times 2\pi/\ell$.

The residual Coulomb interaction H_{I} causes spin-exchange-forces between electrons. The spin-exchange-interaction takes the form $C\left(\sigma_1^{+}\sigma_2^{-} + \sigma_1^{-}\sigma_2^{+}\right)$, where σ^{+} is the

transformation operator from a down-spin state to an up-spin state and σ^- is the Hermitian conjugate operator of σ^+. The coupling constant values of the spin-exchange-interactions are evaluated by integrating transition matrix elements of the residual Coulomb interaction. The detail calculation is shown in Appendix 1. These spin-exchange-interactions produce quantum transitions where the energy before a transition is equal to the energy after a transition - that is to say, the two states are degenerate in H_{D}. Therefore, the spin-exchange interactions should be treated strictly. When we consider the spin-exchange interactions between the nearest-neighbor electrons only, we obtain an approximate Hamiltonian *H*, the explicit form of which is shown in the next section.

We should note that there are two other electron configurations with filling factors of 2/3, apart from that shown in Figure 1.

---------- Fig. 2 ----------

When we move each electron in Figure 1 from its original orbital to the nearest orbital to the left, we obtain the new electron configuration shown in Figure 2a. Figure 2b is created from Figure 2a by the same movement, i.e. one orbital to the left. This movement cannot be produced through the Coulomb interactions, because the three total momenta of the x-direction are different from each other for the three electron configurations. This is verified as follows: we denote the wave number of i-th electron by k_i for Figure 1 and k_i'' for Figure 2b. Then, we can easily see $k_i'' = k_i + 2\pi/\ell$. So, the total momentum of the state shown in Figure 2b is larger than the total momentum of the state shown in Figure 1 by $\left(N\ 2\pi\hbar/\ell\right)$, where N is the total number of electrons. Since the total momentum is conserved in the Coulomb transition, the three states are independent of each other. These states with the electron configurations of Figures 1, 2a and 2b have the same eigenvalue of the Hamiltonian H_{D} neglecting edge effects, and therefore the probabilities of these states

are equal to each other in a thermal equilibrium. Consequently, the equilibrium state has a uniform charge density for large devices where we can neglect the edge effects.

When a quantum Hall device is extremely small, namely with an extremely small width of the direction y and with an extremely small length of the direction x, the intervals between electron orbitals becomes large and also the potentials in the two edges cannot be neglected. Accordingly, only one state in the three electron configurations of Figures 1, 2a and 2b has the minimum energy, and then only the state is realized in a low temperature. In this case, the striped pattern which is created by filled electron orbitals and by empty orbitals may be observed in an appropriate experiment.

3. Spin exchange interaction

We denote the coupling constants of the spin exchange interactions by ξ for an electron pair in the nearest orbitals, and by η for an electron pair in the second nearest orbitals. These coupling constants are evaluated in Appendix 1. Then, we get an approximate Hamiltonian H for the filling factor of 2/3,

$$H = \sum_{j=1,2,3\cdots}\left[\xi\left(\sigma^{+}_{2j-1}\sigma^{-}_{2j}+\sigma^{-}_{2j-1}\sigma^{+}_{2j}\right)+\eta\left(\sigma^{+}_{2j}\sigma^{-}_{2j+1}+\sigma^{-}_{2j}\sigma^{+}_{2j+1}\right)\right]+\sum_{i=1,2,3\cdots}\frac{\mu_{\mathrm{B}}g}{\mu_0}B\frac{1}{2}\sigma^{z}_{i}\,, \quad (5)$$

where g is the g-factor, B is the magnetic field strength, σ^{z} is the electron spin operator in the z-direction, μ_0 is the permeability of vacuum and μ_{B} is the Bohr magneton. The coupling constants ξ and η act between electron pairs as shown in Figure 1. The Hamiltonian of Equation (5) can be diagonalized by using the method in reference [6]. By replacing the down-spin state $|\Downarrow\rangle$ with the vacuum state $|0\rangle$, and the up-spin state $|\Uparrow\rangle$ with a fermion state $c^{*}|0\rangle$, the Hamiltonian (5) can be rewritten in an equivalent form as

$$H = \sum_{j=1,2,3\cdots}\left[\xi\left(c^{*}_{2j-1}c_{2j}-c_{2j-1}c^{*}_{2j}\right)+\eta\left(c^{*}_{2j}c_{2j+1}-c_{2j}c^{*}_{2j+1}\right)\right]+\sum_{i=1,2,3\cdots}\frac{\mu_{\mathrm{B}}g}{\mu_0}B\frac{1}{2}\left(2c^{*}_{i}c_{i}-1\right), \quad (6)$$

where the operators c_i and c_i^* are the annihilation and creation operators of a fermion with site number *i*, and satisfy the anti-commutation relations

$$\{c_i, c_j^*\} = \delta_{i,j}, \ \{c_i, c_j\} = 0, \ \{c_i^*, c_j^*\} = 0 . \quad (7)$$

It should be noted that two minus signs appear in the square brackets of the Hamiltonian (6). When the operator $\left(-c_{2j-1}c_{2j}^*\right)$ acts on the state $c_{2j-1}^*|0\rangle$, we get $\left(-c_{2j-1}c_{2j}^*\right)c_{2j-1}^*|0\rangle = c_{2j}^*|0\rangle$. Thus, the minus signs ensure that the sign of spin states are correct. A unit cell in the Hamiltonian (6) is made of two electrons, and so we can renumber operators c_i and c_i^* using the cell number *j*;

$$a_j = c_{2j-1}, \ b_j = c_{2j}, \ a_j^* = c_{2j-1}^*, \text{ and } b_j^* = c_{2j}^* . \quad (8)$$

This renumbering results in a new Hamiltonian (9),

$$H = \sum_{j=1}^{J}\left[\xi\left(a_j^* b_j - a_j b_j^*\right) + \eta\left(b_j^* a_{j+1} - b_j a_{j+1}^*\right)\right] + \sum_{j=1}^{J}\frac{\mu_B g}{\mu_0} B\frac{1}{2}\left(2a_j^* a_j + 2b_j^* b_j - 2\right), \quad (9)$$

where *J* is the total cell number, $J = N/2$ for *N* the total number of electrons.

4. Solution of eigenvalue problem

We apply a Fourier transformation to the operators a_j, a_j^*, b_j, and b_j^* as follows:

$$a_n = \frac{1}{\sqrt{J}}\sum_p e^{ipn}a(p), \quad b_n = \frac{1}{\sqrt{J}}\sum_p e^{ipn}b(p), \quad (10)$$

where $p = \frac{2\pi}{J} \times \text{integer}$, $-\pi < p \le \pi$. Substituting (10) into (9) then produces

$$H = \sum_p\left[\xi\left(a^*(p)b(p) + b^*(p)a(p)\right) + \eta\left(e^{ip}b^*(p)a(p) + e^{-ip}a^*(p)b(p)\right)\right] + \sum_p\frac{\mu_B g}{\mu_0}B\frac{1}{2}\left(2a^*(p)a(p) + 2b^*(p)b(p) - 2\right) \quad . \quad (11)$$

The Hamiltonian (11) is separated into various terms with different momenta. Hence we can diagonalize the Hamiltonian by solving the eigenvalue problem for the matrix

$$\begin{pmatrix} \frac{\mu_B g}{\mu_0} B & \xi + \eta e^{-ip} \\ \xi + \eta e^{ip} & \frac{\mu_B g}{\mu_0} B \end{pmatrix}. \quad (12)$$

The eigenvalues $\lambda_1(p)$ and $\lambda_2(p)$ are

$$\lambda_1(p) = \frac{\mu_B g}{\mu_0} B - \sqrt{\xi^2 + \eta^2 + 2\xi\eta\cos p}\,, \quad \lambda_2(p) = \frac{\mu_B g}{\mu_0} B + \sqrt{\xi^2 + \eta^2 + 2\xi\eta\cos p}\,. \quad (13)$$

We define new annihilation operators $A_1(p)$ and $A_2(p)$ as

$$A_1(p) = \frac{1}{\sqrt{2}} a(p) - \frac{\xi + \eta e^{-ip}}{\sqrt{2\left(\xi^2 + \eta^2 + 2\xi\eta\cos p\right)}} b(p), \quad (14a)$$

$$A_2(p) = \frac{1}{\sqrt{2}} a(p) + \frac{\xi + \eta e^{-ip}}{\sqrt{2\left(\xi^2 + \eta^2 + 2\xi\eta\cos p\right)}} b(p). \quad (14b)$$

The Hamiltonian (11) can then be rewritten in the diagonal form

$$H = \sum_p \left(\lambda_1(p) A_1^*(p) A_1(p) + \lambda_2(p) A_2^*(p) A_2(p) - \frac{\mu_B g}{\mu_0} B \right). \quad (15)$$

The electron-spin polarization γ_e is defined as the thermo-dynamic mean value

$$\begin{aligned} \gamma_e &= \frac{1}{N}\left\langle -\sum_{i=1}^{N} \sigma_i^z \right\rangle = \frac{-1}{N}\left\langle \sum_{i=1}^{N} \left(2c_i^* c_i - 1\right) \right\rangle = \frac{-1}{N}\left\langle \sum_{j=1}^{J} \left(2a_j^* a_j + 2b_j^* b_j - 2\right) \right\rangle \\ &= \frac{-1}{2J}\left\langle \sum_p \left(2a^*(p)a(p) + 2b^*(p)b(p) - 2\right) \right\rangle = \frac{-1}{2J}\left\langle \sum_p \left(\sum_{s=1}^{2} \left(2A_s^*(p)A_s(p) - 1\right) \right) \right\rangle \end{aligned}, \quad (16)$$

where the minus sign comes from the negative charge of an electron. Since the eigenenergies are 0 and $\lambda_s(p)$ for the states $A_s^*(p)A_s(p) = 0$ and $A_s^*(p)A_s(p) = 1$ respectively, the probabilities of these states are proportional to the Boltzmann factors 1 and $\exp\left(-\lambda_s(p)/k_B T\right)$, where k_B is the Boltzmann constant and T is the temperature. Accordingly, the probability is $\frac{1}{1 + \exp\left(-\lambda_s(p)/k_B T\right)}$ for $A_s^*(p)A_s(p) = 0$, and $\frac{\exp\left(-\lambda_s(p)/k_B T\right)}{1 + \exp\left(-\lambda_s(p)/k_B T\right)}$ for $A_s^*(p)A_s(p) = 1$. These probabilities give the thermo-dynamic mean

value of $A_s^*(p)A_s(p)$,

$$\left\langle A_s^*(p)A_s(p)\right\rangle = \frac{\exp\left(-\lambda_s(p)/k_BT\right)}{1+\exp\left(-\lambda_s(p)/k_BT\right)}, \quad (17)$$

which gives

$$\left\langle 2A_s^*(p)A_s(p)-1\right\rangle = \frac{\exp\left(-\lambda_s(p)/k_BT\right)-1}{1+\exp\left(-\lambda_s(p)/k_BT\right)} = -\tanh\left(\lambda_s(p)/2k_BT\right). \quad (18)$$

Consequently,

$$\gamma_e = \frac{1}{2J}\sum_p\left(\sum_{s=1}^{2}\tanh\left(\lambda_s(p)/2k_BT\right)\right). \quad (19)$$

For a macroscopic number of electrons, we can replace the summation with an integration,

$$\gamma_e = \frac{1}{4\pi}\int_{-\pi}^{\pi}dp\left(\sum_{s=1}^{2}\tanh\left(\lambda_s(p)/2k_BT\right)\right). \quad (20)$$

Thus, we have obtained the electron-spin polarization for the fractional quantum Hall state with a filling factor of 2/3. In the next section we perform the numerical integration.

5. Magnetic behavior of the spin-polarization

An energy gap appears between the two spectra of the eigenvalues $\lambda_1(p)$ and $\lambda_2(p)$. At zero temperature, this gap causes a vanishing of the spin-polarization below some positive value *X* of the magnetic field. When the magnetic field strength increases beyond the value *X*, the spin-polarization increases continuously until reaching the maximum value of 1.

In a real Hall device, random potentials exist. The random potentials produce fluctuations in the eigenvalues of the system. We assume that this effect can be approximated by a thermal fluctuation. We therefore take *T* to be an effective temperature.

Adopting the values $\eta/\xi = 0.25$ and $(k_BT/\xi) = 0.2$, we obtain the magnetic behavior of spin-polarization shown in Figure 3. Experimental data from Kukushkin, Klitzing, and Eberl [5] are also shown in Figure 3.

---------- Fig. 3 ----------

Figure 3 shows that the calculated spin-polarization results are in good accord with the experimental data.

In the next section we examine the magnetic behaviors of the spin-polarization for filling factors other than 2/3.

6. Other filling factors

We now calculate the spin-polarizations for the filling factors 1/2, 3/5, 7/5, 8/5, and 4/7. We first consider the filling factors 3/5 and 4/7. The electron configuration for ν=3/5 is a repetition of the sequence (filled, filled, empty, filled, empty) and that for ν=4/7 is a repetition of the sequence (filled, filled, empty, filled, empty, filled, empty) (see Figures 4a and 4b).

---------- Fig. 4 ----------

These electron configurations produce the minimum classical Coulomb energies. By considering only the spin-exchange interactions between the nearest neighbor electrons, we obtain an approximate Hamiltonian *H* for the filling factors of 3/5, in a form similar to that of the ν=2/3 Hamiltonian (5),

$$H = \sum_{j=1,2,3\cdots}\left[\xi\left(\sigma^{+}_{3j-2}\sigma^{-}_{3j-1}+\sigma^{-}_{3j-2}\sigma^{+}_{3j-1}\right)+\eta\left(\sigma^{+}_{3j-1}\sigma^{-}_{3j}+\sigma^{-}_{3j-1}\sigma^{+}_{3j}\right)+\eta\left(\sigma^{+}_{3j}\sigma^{-}_{3j+1}+\sigma^{-}_{3j}\sigma^{+}_{3j+1}\right)\right]$$
$$+\sum_{i=1,2,3\cdots}\frac{\mu_B g}{\mu_0}B\frac{1}{2}\sigma^{z}_{i} \quad . \qquad (21)$$

Solving the eigenvalue problem for this Hamiltonian (21) by the same method as used in the Hamiltonian (5), we obtain the magnetic-field dependences of the spin-polarizations. The

result for ν =3/5 is shown in Figures 5(a), where we adopt the values $\eta/\xi = 0.25$ and $(k_{\mathrm{B}}T/\xi) = 0.2$, which are the same as in the case of ν =2/3.

----------Fig. 5a ---------- Fig.5b ----------

Similarly, the ν =4/7 Hamiltonian can be obtained, and the calculated result of the spin-polarizations is shown in Figures 5(b). In Appendix 2, we examine how the spin-polarization depends on the parameters η/ξ and $(k_{\mathrm{B}}T/\xi)$.

The minimum Coulomb energy electron configuration for a filling factor of 1/2 is the sequence (filled, empty, filled, empty,...), and consequently all the nearest spin exchange interactions have the coupling constant η only. The calculated spin-polarization for this filling factor is shown in Figure 6

---------- Fig.6 ----------

For filling factors greater than 1, such as 7/5 and 8/5, some orbitals are occupied by two electrons with up and down spins, and the other orbitals are occupied by a single electron. The electron configuration with the minimum Coulomb energy for a filling factor of 8/5 is illustrated in Figure 7.

---------- Fig.7 ----------

The orbitals occupied by a single electron are illustrated by single lines and the orbitals occupied by two electrons with up and down spins are illustrated by double lines. The coupling constants of spin-exchange interactions have the values η' and ς', indicated in Figure 7, where ς' is the coupling constant between an electron pair occupying third nearest orbitals, and the prime indicates that all the orbitals between the interacting pair of electrons are filled with electron pairs with up and down spins. The screening effect of the interposing

electron pairs weakens the coupling constants of the spin exchange interactions. The calculated spin polarizations are shown in the curves in Figures 8(a) and (b) for the filling factors of 7/5 and 8/5.

---------- Fig.8a -------- Fig.8b ----------

Thus, for filling factors greater than 1, the calculated spin-polarizations are also in accord with the experimental data of Kukushkin, et al [5].

7. Conclusion

The magnetic-field dependence of the spin-polarization in FQHE depends strongly on electron configuration. As can be seen in Figures 3, 5, 6, and 8, the fractional quantum Hall states for the filling factors 2/3, 4/7, and 8/5 possess an energy gap between the ground state and the first excited state at zero external field, whereas the states with the filling factors 1/2, 3/5, and 7/5 have no energy gap. These curves are consistent with Haldane's conjecture [7], and are derived from the present theory for spin-chains with two kinds of coupling constants.

Thus, we have satisfactorily reproduced the various experimental spin polarization curves. We note also that, although not presented here, the theoretical values for the filling factors 1/4, 2/5, 3/7, 4/9, 4/3, and 3/2 can also be shown to be in good accord with the experimental data.

There are small shoulders in the experimental curves [5]. A height of a shoulder takes the mean value of the two heights of two horizontal parts appearing in the spin polarization curve. This structure is not explained by the present theory. This problem will be solved in the next paper, where we will take the spin-Peierls-effect into consideration.

References

[1] R. B. Laughlin, Phys. Rev. **B 27** (1983) 3383; Phys. Rev. Lett. **50** (1983) 1395.

F. D. M. Haldane, Phys. Rev. Lett. **51** (1983) 605. B. I. Halperin, Phys. Rev. Lett. **52** (1984) 1583. J. K. Jain, Phys. Rev. Lett. **62** (1989) 199; Phys. Rev. **B 41** (1990) 7653.

[2] R. Tao and D. J. Thouless, Phys. Rev. **B 28** (1983) 1142; R. Tao, Phys. Rev. **B 29** (1984) 636.

[3] S. Sasaki, Physica **B 281** (2000) 838. S. Sasaki, Proc. 25th Int. Conf. Phys. Semicond., Osaka 2000 (Eds. N. Miura and T. Ando) 925.

[4] R. Willet, et al, Phys. Rev. Lett. **59** (1987) 1776.

[5] I. V. Kukushkin, K. v. Klitzing, and K. Eberl, Phys. Rev. Lett. **82**, (1999) 3665.

[6] S. Sasaki, Phys. Rev. **E, 53** (1996) 168.

[7] F. D. M. Haldane, Phys. Rev. Lett. **50** (1983) 1153; Phys. Lett. **93A**, (1983) 464.

Appendix 1

We evaluate a transition matrix element $C(k_1,k_2)$ from an initial state $(k_1,\uparrow;\ k_2,\downarrow)$ to a final state $(k_2,\uparrow;\ k_1,\downarrow)$, as follows:

$$C(k_1,k_2)=$$

$$\iiint\iiint \psi_{k_2}{}^{*}(x_1,y_1,z_1)\psi_{k_1}{}^{*}(x_2,y_2,z_2)\frac{e^2}{4\pi\varepsilon\sqrt{(x_1-x_2)^2+(y_1-y_2)^2+(z_1-z_2)^2}}\times$$

$$\psi_{k_1}(x_1,y_1,z_1)\psi_{k_2}(x_2,y_2,z_2)\,\mathrm{d}x_1\mathrm{d}y_1\mathrm{d}z_1\mathrm{d}x_2\mathrm{d}y_2\mathrm{d}z_2$$

$$= u^4\iint\iint\iint e^{i(k_1-k_2)(x_1-x_2)}\exp\left(-\frac{eB}{2\hbar}\left(y_1-\frac{\hbar k_2}{eB}\right)^2\right)\exp\left(-\frac{eB}{2\hbar}\left(y_2-\frac{\hbar k_1}{eB}\right)^2\right)\phi(z_1)\phi(z_2)\times$$

$$\frac{e^2}{4\pi\varepsilon\sqrt{(x_1-x_2)^2+(y_1-y_2)^2+(z_1-z_2)^2}}\times \qquad ,$$

$$\exp\left(-\frac{eB}{2\hbar}\left(y_1-\frac{\hbar k_1}{eB}\right)^2\right)\exp\left(-\frac{eB}{2\hbar}\left(y_2-\frac{\hbar k_2}{eB}\right)^2\right)\phi(z_1)\phi(z_2)\,\mathrm{d}x_1\mathrm{d}y_1\mathrm{d}z_1\mathrm{d}x_2\mathrm{d}y_2\mathrm{d}z_2$$

where ε is the permittivity of a Hall device. This matrix element means that the spin of the electron in orbital 1 flips from up to down and the spin of the electron in orbital 2 flips from down to up. Therefore, we obtain the spin exchange interaction such as $C(k_1,k_2)\sigma_1{}^{-}\sigma_2{}^{+}$. Similarly, we obtain the interaction $C(k_1,k_2)\sigma_1{}^{+}\sigma_2{}^{-}$ by calculating the transition matrix element from the initial state $(k_1,\downarrow;\ k_2,\uparrow)$ to the final state $(k_2,\downarrow;\ k_1,\uparrow)$.

We adopt a Gaussian form $fe^{-\beta z^2}$ as the wave function of the z-direction $\phi(z)$. (This wave function depends on a potential shape of the z-direction, details of which are unknown.) Substituting this form into the integration in the transition matrix element, we obtain

$$C(k_1,k_2)=(uf)^4\iiint\iiint e^{i(k_1-k_2)(x_1-x_2)}\exp\left(-\frac{eB}{2\hbar}\left(y_1-\frac{\hbar k_2}{eB}\right)^2\right)\exp\left(-\frac{eB}{2\hbar}\left(y_2-\frac{\hbar k_1}{eB}\right)^2\right)\times$$

$$\frac{e^2}{4\pi\varepsilon\sqrt{(x_1-x_2)^2+(y_1-y_2)^2+(z_1-z_2)^2}}\times$$

$$\exp\left(-\frac{eB}{2\hbar}\left(y_1-\frac{\hbar k_1}{eB}\right)^2\right)\exp\left(-\frac{eB}{2\hbar}\left(y_2-\frac{\hbar k_2}{eB}\right)^2\right)e^{-2\beta z_1^2}e^{-2\beta z_2^2}\,\mathrm{d}x_1\mathrm{d}y_1\mathrm{d}z_1\mathrm{d}x_2\mathrm{d}y_2\mathrm{d}z_2$$

$$=(uf)^4\iiint\iiint e^{i(k_1-k_2)(x_1-x_2)}\exp\left(-\frac{eB}{2\hbar}\left(y_1-\frac{\hbar k_2}{eB}\right)^2\right)\exp\left(-\frac{eB}{2\hbar}\left(y_2-\frac{\hbar k_1}{eB}\right)^2\right)\times$$

$$\frac{e^2}{4\pi\varepsilon\sqrt{(x_1-x_2)^2+(y_1-y_2)^2+(z_1-z_2)^2}}e^{-\beta(z_1-z_2)^2}e^{-\beta(z_1+z_2)^2}\times \qquad \text{(A1)}$$

$$\exp\left(-\frac{eB}{2\hbar}\left(y_1-\frac{\hbar k_1}{eB}\right)^2\right)\exp\left(-\frac{eB}{2\hbar}\left(y_2-\frac{\hbar k_2}{eB}\right)^2\right)\mathrm{d}x_1\mathrm{d}y_1\mathrm{d}z_1\mathrm{d}x_2\mathrm{d}y_2\mathrm{d}z_2$$

The coupling constants ξ, η and ζ in sections 3-6 are defined by $C(k_1,k_1+2\pi/\ell)$, $C(k_1,k_1+4\pi/\ell)$ and $C(k_1,k_1+6\pi/\ell)$, respectively. The ratio of the coupling constants η and ξ is given by $\eta/\xi=C(k_1,k_1+4\pi/\ell)/C(k_1,k_1+2\pi/\ell)$. We numerically calculate this ratio by using a computer, where the strength of magnetic field is chosen to be the middle magnitude ($B=5\mathrm{T}$) in the experimental data [5]. Since electrons are scattered by many impurities in a Hall device, the wave function of the x-direction takes a plane-wave form only in an interval between the impurities. Therefore, the length ℓ of the plane wave is not so long. We take the value of ℓ to be $0.1\mu\mathrm{m}$ as an example, and choose the current depth of the z-direction to be $0.001\mu\mathrm{m}$, namely $\sqrt{\beta}=1000[\mu\mathrm{m}]^{-1}$. The value of (A1) weakly depends on the value of β. In the case of $B=5\mathrm{T}$, $\ell=0.1\mu\mathrm{m}$, and $\sqrt{\beta}=1000[\mu\mathrm{m}]^{-1}$, we obtain the ratio $\eta/\xi=0.247$. Therefore, we calculate the spin polarization near the value 0.25 for η/ξ.

Appendix 2

We calculate spin-polarizations for different values of η/ξ in order to examine the dependence on parameters. The results are shown in Figure 9. The calculated spin-polarizations are fairly good agreement with the experimental data, when the value of η/ξ changes from 0.25 to 0.35.

---------- Fig.9 ----------

As is easily seen in those four figures, the change of the value of η/ξ affects the width of the plateau. If another experiment is carried out, the experimental value of the plateau width is probably affected by the shape and by the quality of a Hall device used in the experiment. We already know similar phenomena that the widths of the plateaus in Hall resistance vary with the qualities of Hall devices used in the experiments. Consequently, the weak dependence on the parameters is favorable for explaining variety of data.

Figure captions

Figure 1: Ground state for ν =2/3

Figure 2: Other electron-configurations for ν =2/3

Figure 3: Calculated spin-polarization curve for $\eta/\xi = 0.25$, $(k_B T/\xi) = 0.2$ and experimental data for $\nu = 2/3$

Figure 4: Electron-configurations for ν =3/5 and 4/7

Figure 5a: Spin polarization for ν =3/5, $\eta/\xi = 0.25$, $(k_B T/\xi) = 0.2$

Figure 5b: Spin polarization for ν =4/7, $\eta/\xi = 0.35$, $(k_B T/\xi) = 0.1$

Figure 6: Spin polarization for ν =1/2, $(k_B T/\eta) = 5.5$

Figure 7: Electron configuration for ν =8/5

Figure 8a: Spin polarization for ν =7/5, $\eta'/\xi' = 0.25$, $(k_B T/\xi') = 0.1$

Figure 8b: Spin polarization for ν =8/5, $\zeta'/\eta' = 0.1$, $(k_B T/\eta') = 0.1$

Figure 9: Dependence of spin-polarization curves on parameter values

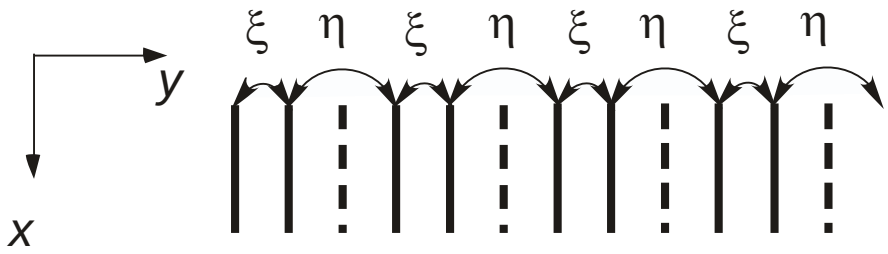

Fig.1

Fig.2a Fig.2b

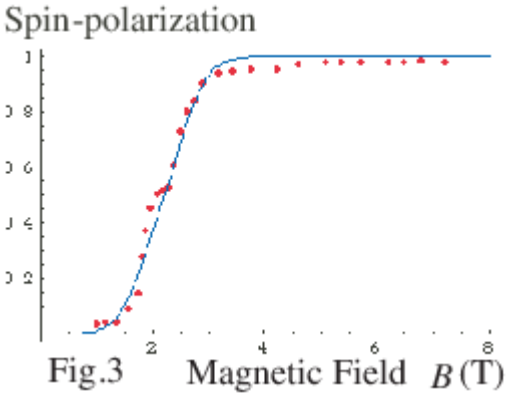

Fig.3 Magnetic Field B (T)

Fig.4a (ν=3/5)

Fig. 4b (ν=4/7)

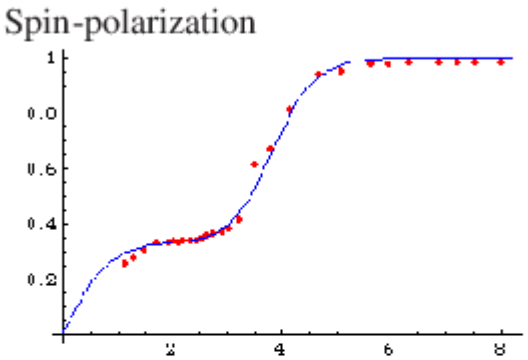

Fig.5a Magnetic Field B (T)

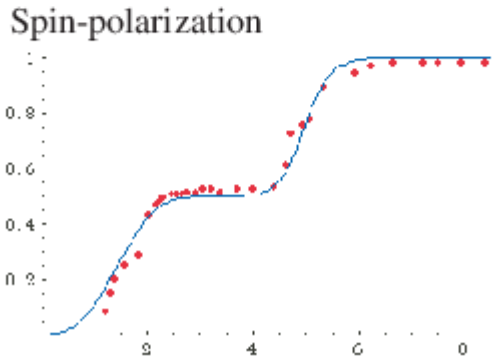

Fig.5b Magnetic Field B (T)

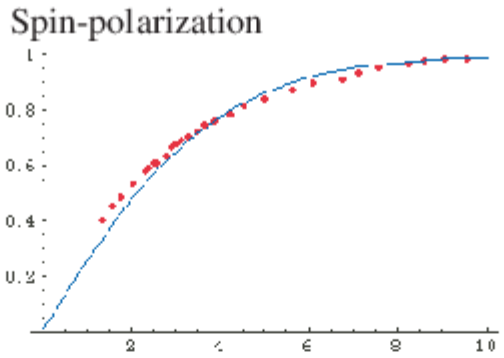

Fig.6 Magnetic Field B (T)

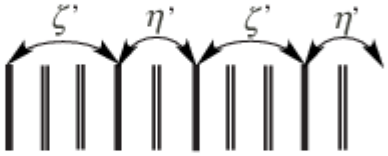

Fig. 7
(ν=8/5)

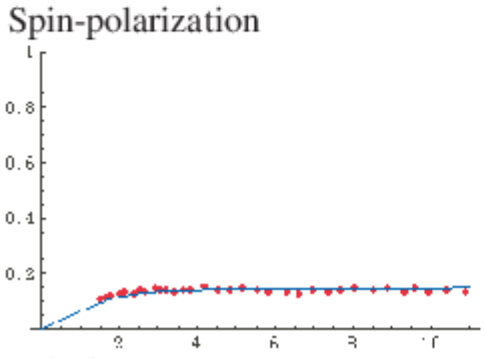

Fig.8a Magnetic Field B (T)

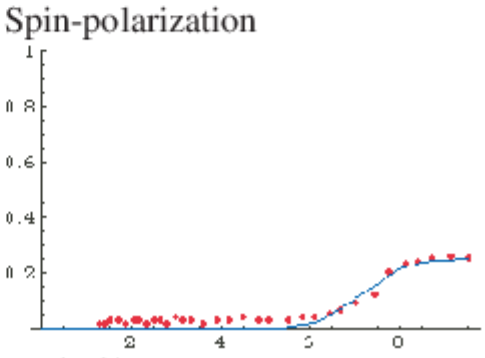

Fig.8b Magnetic Field B (T)

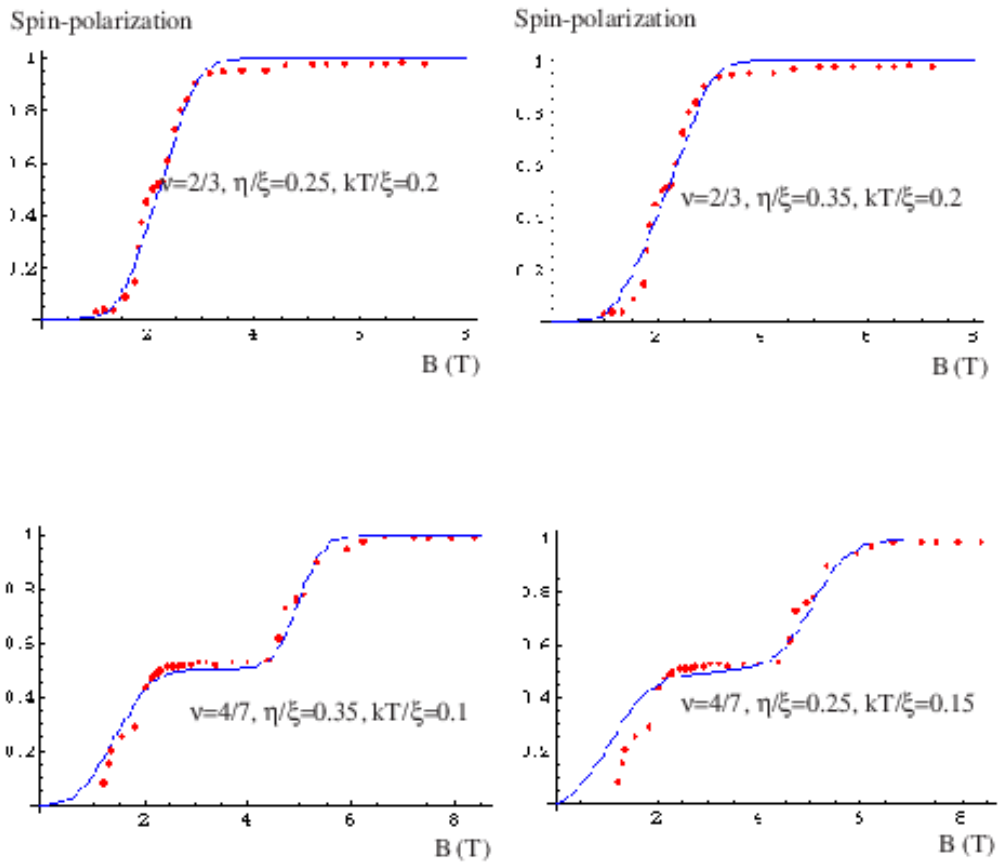
Spin-polarization
ν=2/3, η/ξ=0.25, kT/ξ=0.2
B (T)
Spin-polarization
ν=2/3, η/ξ=0.35, kT/ξ=0.2
B (T)
ν=4/7, η/ξ=0.35, kT/ξ=0.1
B (T)
ν=4/7, η/ξ=0.25, kT/ξ=0.15
B (T)

Fig.9